Average Rician K-Factor-Based Uncertainty Model of Measured Antenna Efficiency Using the Reference Antenna Method in Reverberation Chambers

Wei Xue, Xiaoming Chen, *Senior Member, IEEE*, Yan Yang, Yi Huang, *Fellow*, *IEEE*

***Abstract*—Along several decades of development, many methods based on reverberation chambers (RC) have been proposed for accurate and efficient measurement of antenna efficiency. The standard reference antenna method is applicable for almost all frequency bands of interest and all types of antennas, thus it may well be the most widely applied method in the industry. In this paper, an average Rician K-factor-based uncertainty model for the standard reference antenna method is proposed. It takes both the number of independent samples and the non-ideality of the RC into consideration. Extensive measurements are performed for different RC configurations. It is shown that the newly proposed uncertainty model provides good and stable estimations of the measurement uncertainties for both unloaded and loaded RCs. Moreover, it is experimentally verified that the differences in the radiation characteristics between the reference antenna and the antenna under test have little effect on measurement uncertainty regardless of the loading conditions of the RC. The findings of this work allow more flexible and efficient antenna efficiency measurements, including estimation of the associated uncertainty.**

***Index Terms*—Average Rician K-factor, antenna efficiency, measurement uncertainty, Reference Antenna Method (RAM), Reverberation Chamber (RC).**

I. Introduction

THE reverberation chamber (RC) is an electrically large conducting cavity containing non-symmetric metallic stirrers. Various stirring techniques [1]-[4] are usually combined in order to change the boundary conditions of the RC effectively, aiming to excite as many electromagnetic (EM) modes as possible. Considering the constructive and destructive effects, on average, the EM field within the testing area can be regarded as statistically isotropic and homogeneous [5]. Owning to the RC's particular advantages (e.g., cost-effectiveness, large testing area, and good repeatability), it has been proven a popular testing facility for both electromagnetic compatibility (EMC) testing [6], [7] and over-the-air (OTA) testing [8], [9]. In this work, we will focus on antenna efficiency measurements, which is another important application of RCs.

A. Related Works and Motivation

In the past decades, many RC-based methods have been proposed to determine antenna efficiency in an accurate and efficient way [6], [10]-[16]. Most of these methods make use of a reference antenna with known efficiency, yet some of them do not. It is worth stressing that getting rid of the dependence on the reference antenna provides not only the convenience, but also some limitations and other prerequisites. For example, the one- and two-antenna methods have specific prerequisites on the enhanced backscatter coefficient (which may not be met in practice, especially for higher frequencies) [17], [18], whereas the three-antenna method needs two additional antennas working at the same frequency range as the antenna under test (AUT). Nevertheless, since the standard reference antenna method is widely used in the industry, and is applicable for almost all types of antennas, we prefer to study the standard reference antenna method here.

Due to the stochastic nature of the RC-based measurements, uncertainty analysis is always a significant and hot issue in this context. Extensive studies have been performed to evaluate the uncertainty of RC-based antenna efficiency measurements, in both semi-empirical and statistical ways [10], [19]-[22]. For the standard reference antenna method, the measurement uncertainty is approximated using the standard derivation based on first-order Taylor expansion described in [19]. The probability density function (PDF) and the related statistics (e.g. expectation, variance, and mean square error) have been derived in [20], which makes the standard reference antenna method consistent complete enough from the viewpoint of statistics.

It should be noted that both the approximated and the statistical uncertainty models were derived based on a prerequisite, that is, the RC is well-stirred. Specifically, the distribution of the electric strength of any rectangular

This work was supported in part by the National Natural Science Foundation of China under Grant 62171362. (*Corresponding author: Xiaoming Chen*)

W. Xue and Y. Yang are with the School of Electronics and Information, Northwestern Polytechnical University, Xi'an 710072, China.

X. Chen is with the School of Information and Communications Engineering, Xi'an Jiaotong University, Xi'an 710049, China (e-mail: xiaoming.chen@mail.xjtu.edu.cn).

Y. Huang is with the Department of Electrical Engineering and Electronics, University of Liverpool, Liverpool L69 3GJ, U.K.

This article has been accepted for publication in a future issue of this journal, but has not been fully edited. Content may change prior to final publication. Citation information: DOI 10.1109/TIM.2021.3132991, IEEE Transactions on Instrumentation and Measurement

component within the working volume must follow an ideal Rayleigh distribution. However, the distribution in a practical RC may become a Rician distribution due to the non-zero unstirred power, which makes the prerequisite unmet. In other words, the existing uncertainty models are limited and cannot cope with the condition of a non-ideal Rayleigh distribution. Moreover, these uncertainty models depend only on the number of independent samples, while ignoring the differences between the reference antenna and the AUT measurements caused by the antenna characteristics (e.g. radiation pattern [23]). These difficulties motivated us to explore a universal uncertainty model for the standard reference antenna method.

B. Approach and Contributions

The Rician K-factor is defined as the ratio of the unstirred power to the stirred power. Obviously, the K-factor is an ideal parameter which allows evaluation of the non-ideality of a practical RC. The measurement uncertainty has been studied preliminarily based on the K-factor [24]-[26]. Since the K-factor is sensitive to the configuration of antennas setup (e.g. orientation and location), two facts must be taken into consideration: 1) the K-factor measured from a single case is only suitable for a specific measurement setup and 2) the true value of K-factor varies as actual source stirring is adopted. Therefore, the average K-factor (K_{avg}) [24], [27] is chosen to improve the applicability of the uncertainty model.

In this work, we use K_{avg} measured for both reference antenna and AUT measurements in order to quantify the corresponding measurement uncertainties, respectively. The total measurement uncertainty is further derived according to the law of propagation of uncertainty [28]. By doing so, both the non-ideality of the RC and the antenna characteristics are taken into consideration.

Compared with previous researches, this work provides three significant contributions: 1) a universal uncertainty model for the standard reference antenna method is proposed, which takes the number of independent samples, the non-ideality of the RC and the antenna characteristics into consideration; 2) extensive RC-based measurements are performed, not only validating the proposed uncertainty model, but also providing comprehensive comparisons between different uncertainty models and measurement setups; 3) it is experimentally verified that the differences in the radiation characteristics between the reference antenna and the AUT have little effect on the measurement uncertainty, which is useful for the RC measurements when trying to characterize the power transfer function (PTF).

In Section II, we give a brief introduction to K_{avg} and we derive the K_{avg}-based uncertainty model. Extensive RC-based measurements are performed in Section III, where comprehensive comparisons and discussions are also given. Section IV concludes this paper with some conclusions.

II. Theoretical Model

For the sake of completeness and in order to facilitate the derivation of the uncertainty model, the average K-factor and the standard antenna method are briefly introduced below.

A. Average K-factor

A typical setup for measurement of antenna efficiency measurement using the standard reference antenna method is depicted in Fig. 1. A two-port Vector Network Analyzer (VNA) is utilized to measure complex Scattering parameters (*S*-parameters). The complex channel transfer function (i.e., transmission parameter S_{21}) measured at mth mechanical stirrer position, sth antenna location and fth working frequency can be modeled as

$$S_{21}(m,s,f) = S_{21,uns}(m,s,f) + S_{21,sti}(m,s,f) \tag{1}$$

where $S_{21,uns}$ and $S_{21,sti}$ represent the unstirred and stirred parts, respectively. For a specific antenna location, $S_{21,uns}$ is deterministic and independent of the stirrer position, while $S_{21,sti}$ varies as the stirrer rotates.

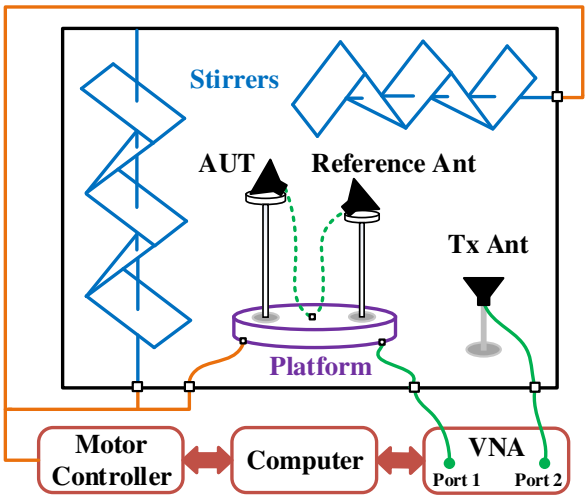

Fig. 1. Measurement setup for the standard reference antenna method.

Note that both the real and imaginary parts of $S_{21,sti}$ follow independent Gaussian distributions with zero mean and the same standard deviation [29], [30], therefore, we can obtain

$$\begin{aligned} S_{21,uns}(s,f) &= \langle S_{21}(m,s,f)\rangle_{N_M} \\ S_{21,sti}(m,s,f) &= S_{21}(m,s,f) - \langle S_{21}(m,s,f)\rangle_{N_M} \end{aligned} \tag{2}$$

where $\langle\bullet\rangle_{N_M}$ denotes the ensemble average over N_M mechanical stirring samples.

Once we obtain the unstirred and stirred power, the measured K-factor can be expressed as

$$K(s,f) = \frac{P_{uns}(s,f)}{P_{sti,avg}(s,f)} = \frac{|S_{uns}(s,f)|^2}{|\langle S_{sti}(m,s,f)\rangle_{N_M}|^2} \tag{3}$$

It is obvious that the unstirred path will be different for different antenna locations or orientations. As a result, the K-factor estimated from a single measurement is meaningless when the antenna configuration changes, e.g. the orientations of the reference antenna and the AUT are different (c.f. Fig. 1), and source stirring is applied. In these cases, it is preferable to use K_{avg} instead of a single K-factor.

$$K_{avg}(f) = \frac{\langle P_{uns}(s,f)\rangle_{N_S}}{\langle P_{sti,avg}(s,f)\rangle_{N_S}} \tag{4}$$

where N_S represents the number of source stirring samples. It

should be stressed that $K_{avg}(f)$ is calculated as the ratio of the average unstirred power to the average stirred power, and not as the average of N_S K-factor. This is mainly because $P_{sti,avg}$ should be a constant and independent of the antenna locations and orientations [27]. If frequency stirring is considered [3], [31], P_{uns} and $P_{sti,avg}$ can be averaged over both N_S source stirring samples and N_F frequency stirring samples.

B. Average K-factor-Based Uncertainty Model

The standard reference antenna method requires two separate RC measurements, i.e., a reference measurement and a measurement of the AUT. The reference measurement is performed between the reference antenna and the transmitting antenna, with the aim to characterize the PTF of the chamber. The AUT measurement is performed between the AUT and the transmitting antenna. During the whole measurement procedure, the objects in the RC should remain unchanged in order to ensure the same loading condition.

According to Hill's equation [5], the PTFs measured for the reference measurement (T_{REF}) and for the AUT measurement (T_{AUT}) should be the same, that is

$$\frac{\langle |S_{21,AUT}|^2 \rangle}{\eta_{AUT}} = T_{AUT} = T_{REF} = \frac{\langle |S_{21,REF}|^2 \rangle}{\eta_{REF}} \tag{5}$$

where η_{AUT} and η_{REF} represent the total efficiency of AUT and reference antenna, respectively. $S_{21,AUT}$ and $S_{21,REF}$ represent the S_{21} determined with the AUT and with the reference antenna, respectively.

Based on (5), η_{AUT} can be obtained as

$$\eta_{AUT} = \frac{\langle |S_{21,AUT}|^2 \rangle}{\langle |S_{21,REF}|^2 \rangle} \eta_{REF} \tag{6}$$

To show the uncertainty analysis clearly and intuitively, we denote $X = \langle |S_{21,AUT}|^2 \rangle$ and $Y = \langle |S_{21,REF}|^2 \rangle$. Considering that η_{REF} is a constant, the relative uncertainty of η_{AUT} can be calculated as

$$\tilde{u}_{K_{avg}}[\eta_{AUT}] = \sqrt{\tilde{u}^2[X] + \tilde{u}^2[Y]} \tag{7}$$

Assume that we have N_M independent mechanical stirring samples and N_S independent source stirring samples, whereas the measurement noise can be ignored, under these conditions the relative uncertainty of the average measured power can be modeled as [25]

$$\tilde{u} = \frac{\sqrt{\frac{1}{N_M N_S} + \frac{2}{N_M N_S} K_{avg} + \frac{1}{N_S} K_{avg}^2}}{1 + K_{avg}} \tag{8}$$

Note that K_{avg} is used in Eq. (8), therefore, Eq. (8) can handle different combinations of antenna locations and orientations.

The relative uncertainties of X and Y can be calculated using Eq. (8), therefore, the relative uncertainty of η_{AUT} can be obtained based on (7)

$$\tilde{u}_{K_{avg}}[\eta_{AUT}] = \sqrt{\frac{\frac{1}{N_M N_S} + \frac{2}{N_M N_S} K_{avg,REF} + \frac{1}{N_S} K_{avg,REF}^2}{(1 + K_{avg,REF})^2} + \frac{\frac{1}{N_M N_S} + \frac{2}{N_M N_S} K_{avg,AUT} + \frac{1}{N_S} K_{avg,AUT}^2}{(1 + K_{avg,AUT})^2}} \tag{9}$$

where $K_{avg,REF}$ and $K_{avg,AUT}$ represent K_{avg} determined with the reference antenna and with the AUT, respectively. Obviously, the effects caused by the differences in antenna characteristics can be reflected in the average K-factor-based uncertainty model.

It is worth noting that in the uncertainty model (9), the stirring sequences for both the reference antenna and the AUT measurements are assumed to be the same, which implies the same number of independent samples. Of course, the uncertainty model (9) can be easily modified with different values for N_M and N_S in reference and AUT measurements.

Here, we consider two special cases: 1) a well-stirred RC and 2) the case where the reference antenna and the AUT have the same characteristics as regards K_{avg}. Firstly, in a well-stirred RC, the power is fully stirred utilizing various stirring techniques. As a result, the unstirred power approximates 0, that is, $K_{avg} = 0$. The uncertainty model (9) reduces to

$$\tilde{u}_{K_{avg}}[\eta_{AUT}] = \sqrt{\frac{2}{N_M N_S}} \tag{10}$$

Then, we suppose that K_{avg} as determined with the reference antenna and with the AUT are the same, that is, $K_{avg,REF} = K_{avg,AUT} = K_{avg}$. Under these conditions the uncertainty model (9) reduces to

$$\tilde{u}_{K_{avg}}[\eta_{AUT}] = \sqrt{2 \times \frac{\frac{1}{N_M N_S} + \frac{2}{N_M N_S} K_{avg} + \frac{1}{N_S} K_{avg}^2}{(1 + K_{avg})^2}} \tag{11}$$

Finally, an extremely large K_{avg} indicates us that most of the power is not being efficiently stirred and that the uniformity of the RC is rather poor. In such an RC environment, the antenna efficiency cannot be measured accurately, therefore, the discussion in this case is meaningless, and shall therefore be omitted.

C. Comparison with the Ideal Theoretical Uncertainty Model

The PDF and associated statistics of the reference antenna method have been derived in [20]. Therefore, the corresponding relative uncertainty model can be easily obtained based on the standard derivation and expectation

$$\tilde{u}_{ideal}[\eta_{AUT}] = \sqrt{\frac{2N_M N_S - 1}{N_M N_S (N_M N_S - 2)}} \tag{12}$$

Again, it should be stressed that the uncertainty model (12) is obtained under ideal conditions, that is, the measured power samples are independently and identically distributed following an exponential distribution.

When N is large, we can apply the following approximation

This article has been accepted for publication in a future issue of this journal, but has not been fully edited. Content may change prior to final publication. Citation information: DOI 10.1109/TIM.2021.3132991, IEEE Transactions on Instrumentation and Measurement

$$\lim_{N\to\infty} \tilde{u}_{ideal}\left[\eta_{\mathrm{AUT}}\right] = \sqrt{\frac{2}{N_{\mathrm{M}} N_{\mathrm{S}}}} \tag{13}$$

Coincidentally, Eqs. (10) and (13) are the same. This should not come as a surprise. The reason is that uncertainty models are obtained under the assumption of a well-stirred RC environment. Meanwhile, approximations are both adopted.

In order to perform a comprehensive and intuitive comparison between the average K-factor-based uncertainty model [i.e., Eq. (9)] and the ideal theoretical uncertainty model [i.e., Eq. (12)], the relative uncertainty model (9) of two case studies are considered, i.e., $K_{avg,\mathrm{REF}} = K_{avg,\mathrm{AUT}}$ and $K_{avg,\mathrm{REF}} > K_{avg,\mathrm{AUT}}$. Focusing on Eq. (9), it is easy to conclude that the analyses of $K_{avg,\mathrm{REF}} > K_{avg,\mathrm{AUT}}$ and $K_{avg,\mathrm{REF}} < K_{avg,\mathrm{AUT}}$ are equivalent. For simplicity and without loss of generality, let us state $K_{avg,\mathrm{REF}} = 1.5 \times K_{avg,\mathrm{AUT}}$ is adopted for case study $K_{avg,\mathrm{REF}} > K_{avg,\mathrm{AUT}}$.

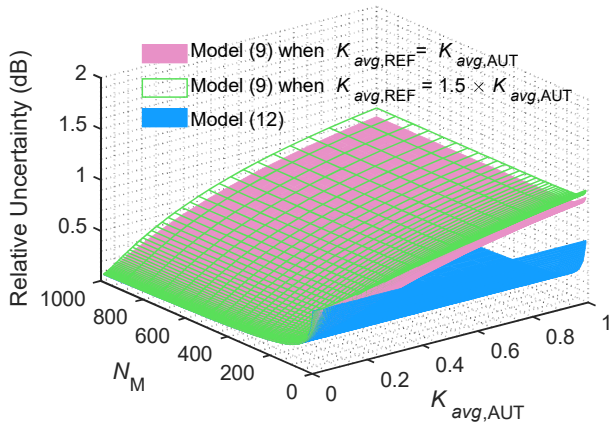

(a)

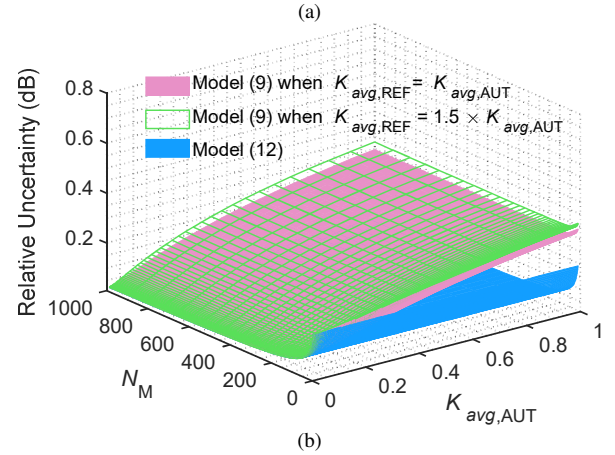

(b)

Fig. 2. Relative uncertainty model (9) of two cases and model (12) when $N_{\mathrm{M}} \in [1, 10^3]$, $K_{avg} \in [10^{-3}, 10^0]$, (a) $N_{\mathrm{S}} = 9$, and (b) $N_{\mathrm{S}} = 100$.

Figure 2 shows the relative uncertainty model (9) for the two case studies and model (12) as a function of N_{M} and K_{avg} when $N_{\mathrm{S}} = 9$ and $N_{\mathrm{S}} = 100$. The relative uncertainties are shown in logarithmic (dB) form, while N_{M} and K_{avg} are shown in linear form. As it can be seen from Fig. 2 (a), the relative uncertainties of the three case studies are comparable to each other when $K_{avg,\mathrm{AUT}}$ approximates 0. However, the discrepancy between model (9) and (12) increases rapidly as $K_{avg,\mathrm{AUT}}$ increases regardless of N_{M}. If $K_{avg,\mathrm{AUT}}$ is large, the increase of N_{M} causes little improvement on the relative uncertainty of model (9), which is totally different from model (12). As a result, the discrepancy between the two models is still obvious even when $N_{\mathrm{M}} = 1000$. For the two case studies of model (9), the case study of larger K_{avg} shows a larger overall uncertainty regardless of N_{M}.

Comparing between Figs. 2(a) and 2(b), it can be seen that the relative uncertainty of the three cases is much decreased as N_{S} increases from 9 to 100. However, the obvious discrepancy between model (9) and (12) can still be observed, as well as the discrepancy between the two cases of model (9). It can be concluded that a simple increase in the number of independent samples cannot offset the uncertainty caused by the K-factor. Therefore, the effects of K-factor must be considered for rigorous uncertainty analysis.

TABLE I
SPECIFIC VALUES OF THE MEASUREMENT UNCERTAINTIES CALCULATED FROM THREE CASE STUDIES: TWO OF MODEL (9) AND ONE OF MODEL (12)

N_{S}	$K_{avg,\mathrm{AUT}}$	N_{M}	Case Study 1 of Model (9) (dB)	Case Study 2 of Model (9) (dB)	Model (12) (dB)
9	0.1	100	0.27	0.30	0.20
		1000	0.19	0.23	0.06
	0.6	100	0.88	0.94	0.20
		1000	0.71	0.80	0.06
100	0.1	100	0.08	0.09	0.06
		1000	0.06	0.07	0.02
	0.6	100	0.28	0.30	0.06
		1000	0.23	0.26	0.02

The specific values of the measurement uncertainties calculated from two case studies of model (9) and model (12) are summarized in Table I. As expected, the discrepancy between the two models increases as $K_{avg,\mathrm{AUT}}$ becomes larger, and the case study with a larger $K_{avg,\mathrm{AUT}}$ shows a higher uncertainty. Comparing the uncertainties of different combinations of N_{S} and N_{M}, it can be found that the measurement uncertainty decreases rapidly as N_{S} or N_{M} increases when they are relatively small. However, significant improvement on the uncertainty becomes impossible as N_{S} or N_{M} increases to a large value. Therefore, it is difficult to achieve a desirable uncertainty level by singly increasing N_{S} or N_{M}, especially for the cases of large $K_{avg,\mathrm{AUT}}$. In other words, both N_{S} and N_{M} should be sufficiently large for an accurate measurement in an imperfect RC.

III. MEASUREMENTS, ANALYSES AND DISCUSSIONS

In order to verify the proposed uncertainty model and to illustrate the effects of K-factor, extensive RC-based measurements are performed. The corresponding analyses and discussions are also given in this section.

A. Measurement Setup and Configurations

Figure 3 shows a photograph of the RC setup for

This article has been accepted for publication in a future issue of this journal, but has not been fully edited. Content may change prior to final publication. Citation information: DOI 10.1109/TIM.2021.3132991, IEEE Transactions on Instrumentation and Measurement

measurement of antenna efficiency using the reference antenna method. The RC has inner dimensions of 1.50 m × 1.44 m × 0.92 m and contains two metallic stirrers (one horizontal and one vertical). A turntable platform is also equipped in the RC for source stirring. Two trestles with adjustable orientation and height are used to support the reference antenna and the AUT. A double-ridged horn antenna works as the transmitting antenna and is located at a fixed position (as shown in Fig. 3). A second double-ridged horn antenna and a discone antenna are selected as the AUT (one directional and one omnidirectional). In order to explore the effect of the differences in antenna characteristics between the reference and the AUT measurements, a third double-ridged horn antenna and a second discone antenna play the role of the reference antenna. In such a configuration, we need to perform twice the reference measurements and twice the AUT measurements for a complete run of the measurement procedure. The antennas connected to the VNA are located more than one wavelength (computed at the lowest testing frequency) away from the nearest metallic objects. The antennas not connected to the VNA are connected to a 50-ohm load.

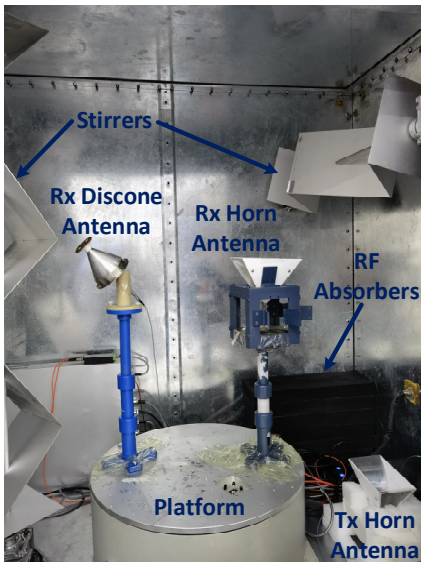

Fig. 3 Photograph of the RC setup for measurement of antenna efficiency using the reference antenna method.

During the whole measurement procedure, the platform rotates step-wisely around 10 positions that are evenly distributed between 0° and 360°. At each platform stirring position, the two stirrers rotate simultaneously and step-wisely around 10 positions that are evenly distributed between 0° and 360°. The *S*-parameters at each stirring position are measured by the VNA from 2 GHz to 3 GHz in 1 MHz step. Therefore, we have in total 100 stirring samples for each reference or AUT measurement.

Considering independent realizations are necessary to calculate the relative uncertainty, therefore, the nine-case uncertainty assessment procedure [6], [24], [26] is utilized here. Specifically, each reference or AUT measurement is repeated for nine different RC configurations: adjusting the trestle to three heights (i.e., 15 cm, 30 cm, and 45 cm) and orientating the antenna on the trestle along three orthogonal directions. The distance between two adjacent heights is far larger than a half-wavelength at 2 GHz and the selected three orientations are orthogonal, thus the nine measurements are theoretically independent from each other.

In this work, the antenna efficiency needs to be measured in different K-factor environments. Due to the platform stirring and the nine-case measurement procedure, K-factor cannot be easily controlled by simply adjusting the alignment between the transmitting and receiving antennas. Therefore, the loading method is adopted in order to tune the K-factor. Each antenna efficiency measurement is performed in an unloaded as well as in a loaded RC. For the loaded RC, six absorbers with the same dimension (16 cm × 5 cm × 48 cm) are stacked at the corner of the RC (c.f. Fig. 3). Note that all the antennas and supporters are placed in the RC during the whole measurement procedure, under both unloaded and loaded conditions.

B. Parameter Determination

As it can be seen from Section II, the proposed uncertainty model is a function of the number of independent samples (i.e., N_M and N_S) and of average K-factors (i.e., $K_{avg,REF}$ and $K_{avg,AUT}$). Therefore, it is essential to have an accurate estimation of the related parameters for determination of the relative uncertainties.

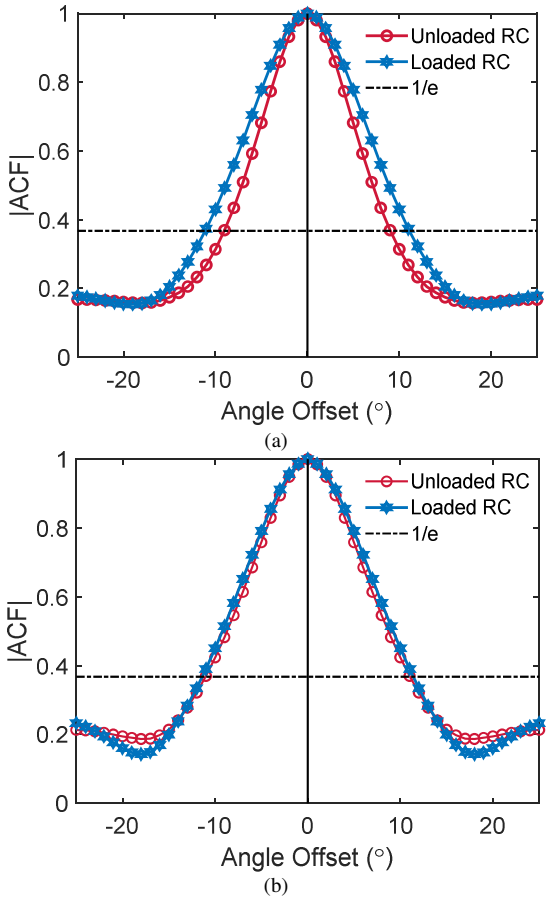

Fig. 4 Magnitude of the complex autocorrelation coefficient of (a) stirrer samples and (b) platform samples as a function of the angle offset.

This article has been accepted for publication in a future issue of this journal, but has not been fully edited. Content may change prior to final publication. Citation information: DOI 10.1109/TIM.2021.3132991, IEEE Transactions on Instrumentation and Measurement

In order to show the correlations between the stirring samples with high precision, an angle step of 1° between samples is considered for both unloading and loading conditions. The autocorrelation coefficients of the stirring samples can be calculated using [6]

$$\mathrm{ACF}(\delta)=\frac{\sum_{i=1}^{N}(S_{21}(i)-\langle S_{21}\rangle)(S_{21}(i+\delta)-\langle S_{21}\rangle)}{\sum_{i=1}^{N}(S_{21}(i)-\langle S_{21}\rangle)^2} \tag{14}$$

where $S_{21}(i)$ represents the ith item of the measured S_{21} sequence, and $S_{21}(i+\delta)$ is the ith item of the measured S_{21} sequence after it is shifted for δ positions. Note that once the autocorrelation coefficients are obtained through Eq. (14), the number of independent samples (i.e., N_M and N_S) can be easily calculated using the autocorrelation function (ACF) estimator. Therefore, the autocorrelation coefficients computed for a given shifting δ is denoted as $\mathrm{ACF}(\delta)$.

Figure 4 shows the autocorrelation coefficients calculated using the stirrer and platform samples for both loaded and unloaded conditions of the RC. In order to avoid the instability caused by the stochastic nature of RC, the autocorrelation coefficients are averaged over a central frequency of 50 MHz. Here, we take e^{-1} (≈ 0.37) as the reference threshold [6] to determine the coherence angle. For the stirrer samples, the coherence angle increases from 9° to 12° as the RC is loaded with absorbers. However, for the platform samples, the coherence angle is approximately 11° for both loading conditions. Nevertheless, it is confirmed that the 10 stirrer samples and the 10 platform samples utilized in the measurements are independent of each other, i.e., $N_M = 10$ and $N_S = 10$.

If frequency stirring is also considered, the number of independent frequency stirring samples (i.e., N_F) can be estimated as

$$N_F=\frac{\mathrm{BW_{fs}}}{B_C} \tag{15}$$

where $\mathrm{BW_{fs}}$ represents the bandwidth used for frequency stirring. B_C represents the coherence bandwidth, which is defined as the frequency range over which the magnitude of the autocorrelation coefficient drops from 1 to a specific value (e.g., 0.5) [24], [32]. The autocorrelation coefficient can be calculated as

$$\rho_f(\Delta f)=\frac{\langle S_{21}^*(f)S_{21}(f+\Delta f)\rangle}{\langle|S_{21}(f)|^2\rangle} \tag{16}$$

where the superscript * denotes the complex conjugate operator. Δf represents the frequency separation and the averaging is performed over all measured stirring samples.

The magnitude of the complex autocorrelation coefficients for both loading conditions as function of frequency separation at $f = 2.5$ GHz is shown in Fig. 5. For both loading conditions, $|\rho_f(\Delta f)|$ decreases as frequency separation is increased. If 0.5 is adopted as the threshold, B_C is about 2.7 MHz and 4.8 MHz for the unloaded and loaded RC, respectively. In addition, we have calculated $|\rho_f(\Delta f)|$ over the entire testing frequency range, and have found that $|\rho_f(\Delta f)|$ fluctuates slightly as the frequency is varied for both loading conditions. In other words, $|\rho_f(\Delta f)|$ nearly remains constant for each loading condition, regardless of frequency. In fact, it has been shown that B_C is independent on frequency for a given RC configuration [24]. Hence B_C can be regarded as a constant over the whole testing bandwidth as well. Nevertheless, N_F can be easily calculated once B_C is determined.

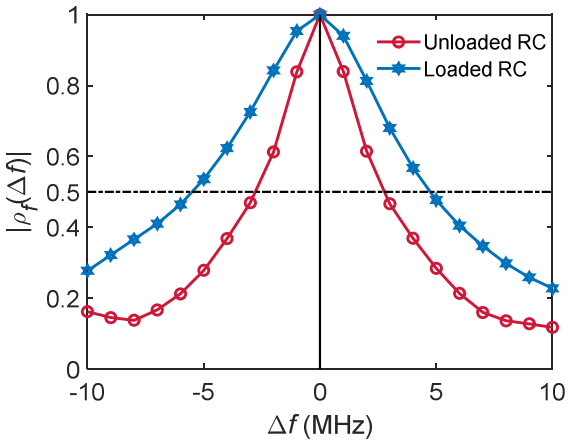

Fig. 5 Magnitude of the complex autocorrelation coefficient as a function of frequency separation at $f = 2.5$ GHz.

In order to perform a full analysis of K_{avg}, the distributions of K_{avg} obtained from three different sample sets in both loading conditions are considered, i.e., (a) a single measurement using the discone antenna, (b) nine measurements using the discone antenna, and (c) nine measurements using the horn antenna. The corresponding results are shown in Fig. 6. As it can be seen from Fig. 6(a), K_{avg} in the loaded RC is larger than that in the unloaded RC, which seems obvious. Since the PDF is obtained from only one single measurement, some discontinuities in the empirical histograms can be observed. When nine measurements are all considered, the PDF becomes much smoother and more stable. For the samples obtained using the horn antenna, K_{avg} in the loaded RC is larger than that in the unloaded RC as well.

Comparing between Figs. 6 (b) and (c), the PDFs for the unloaded RC are approximately the same. However, for the loaded RC, the PDF obtained using the horn antenna shows a slight shift to the left. That is, the expectation of K_{avg} for the horn antenna is smaller than that for the discone antenna. Based on the definition of K_{avg}, it is believed that the discrepancies between these two PDFs are mainly caused by the differences in the antenna radiation characteristics. Nevertheless, if the K_{avg}-based uncertainty model is adopted to determine the measurement uncertainty, these discrepancies can be fully taken into account.

C. Analysis of Relative Uncertainties

Figure 7 shows the empirical and analytical relative uncertainties of the discone and the horn antennas using different reference antennas in an unloaded RC. Since the K_{avg} factor of the discone and the horn antennas are different, the

This article has been accepted for publication in a future issue of this journal, but has not been fully edited. Content may change prior to final publication. Citation information: DOI 10.1109/TIM.2021.3132991, IEEE Transactions on Instrumentation and Measurement

corresponding relative uncertainties should be calculated separately. In addition, the uncertainty model (12) is also shown in the figure for comparison. Since K_{avg} of the discone and the horn antennas are almost the same for the unloaded RC, the uncertainties (9) calculated using different reference antennas are approximately the same as well. Note that both $K_{avg,\mathrm{REF}}$ and $K_{avg,\mathrm{AUT}}$ are relatively small for the unloaded RC, thus the theoretical uncertainties of models (9) and (12) are close to each other.

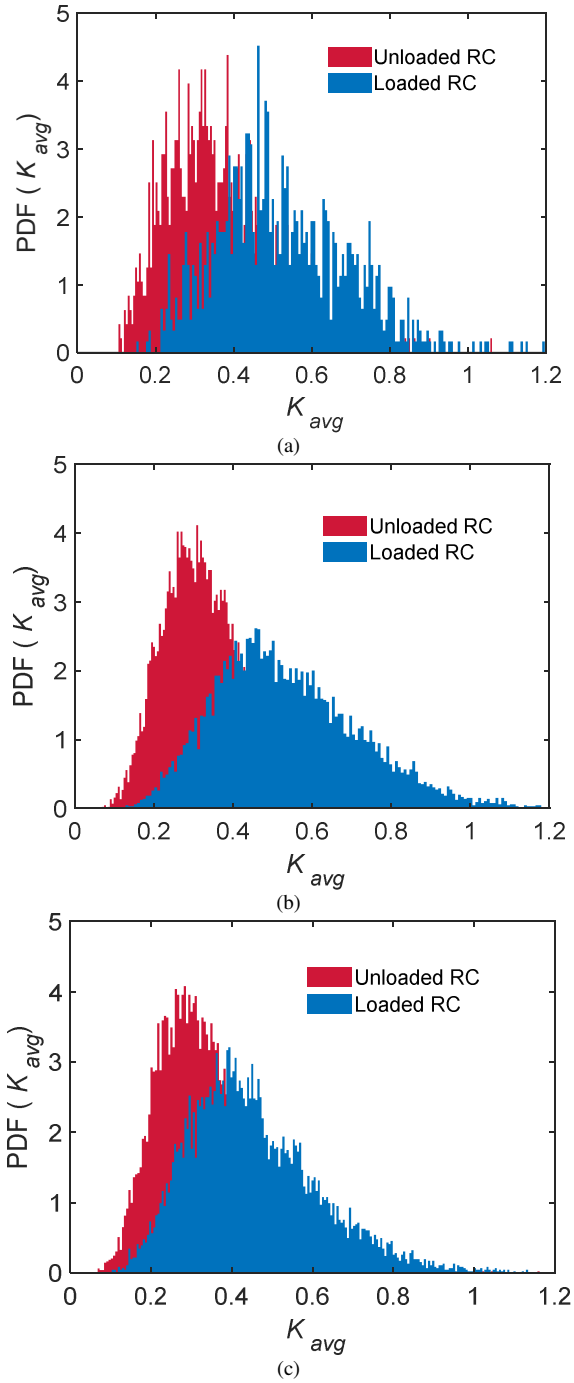

Fig. 6 Distributions of the average K-factor for both unloaded and loaded conditions of the RC when $N_{\mathrm{M}} = 100$ over 1 GHz for three cases: (a) Measured using the discone antenna for $N_{\mathrm{S}} = 1$ times. (b) Measured using the discone antenna for $N_{\mathrm{S}} = 9$ times. (c) Measured using the horn antenna for $N_{\mathrm{S}} = 9$ times.

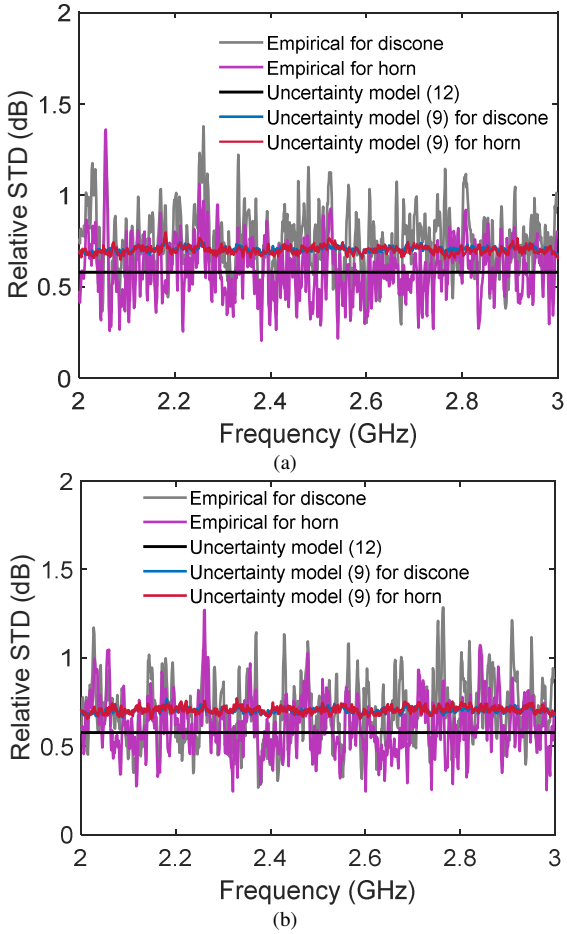

Fig. 7 Empirical and analytical relative uncertainties of the discone and the horn antennas in an unloaded RC when using (a) a horn antenna and (b) a discone antenna as the reference antenna.

Compared with the uncertainty model (9), the uncertainty model (12) shows better performance at some specific frequencies, while generally its overall performance is a little worse. Specifically, the uncertainty model (9) suffers from a slight underestimation of the empirical relative uncertainty. This is mainly due to the actual imperfections of the RC which are encountered in practice. The derivation of the uncertainty model (9) has an important prerequisite, i.e. that the PTF of the RC must follow an ideal exponential distribution. Obviously, this requisite may not be completely met in practical measurements, which leads to a slight underestimation.

Figure 8 shows the empirical and analytical relative uncertainties of the discone and the horn antennas using different reference antennas in a loaded RC. Comparing between Figs. 7 and 8, the empirical relative uncertainties exhibit a slight increase for both AUT. Due to the absorbers loaded in the RC, the field uniformity suffers from deterioration to a certain extent. This explains why the uncertainty for the loaded RC is higher than that for the unloaded RC. As discussed in Section III.B, the selected 100 stirring samples are completely independent for both the unloaded and loaded RC, which means that the uncertainty model (9) provides the same uncertainties for both loading conditions. As a result, the

This article has been accepted for publication in a future issue of this journal, but has not been fully edited. Content may change prior to final publication. Citation information: DOI 10.1109/TIM.2021.3132991, IEEE Transactions on Instrumentation and Measurement

uncertainty model (9) provides an obvious underestimation of the empirical relative uncertainties for the loaded RC. By comparison, the uncertainties determined with model (12) increase as K_{avg} is increased when absorbers are loaded in the RC (cf. Fig. 6). We can see from Fig. 8 that the empirical relative uncertainties are in accordance with the uncertainty model (12) for both the discone and the horn AUT. However, obvious discrepancies between the empirical relative uncertainties and the uncertainty model (12) can be observed.

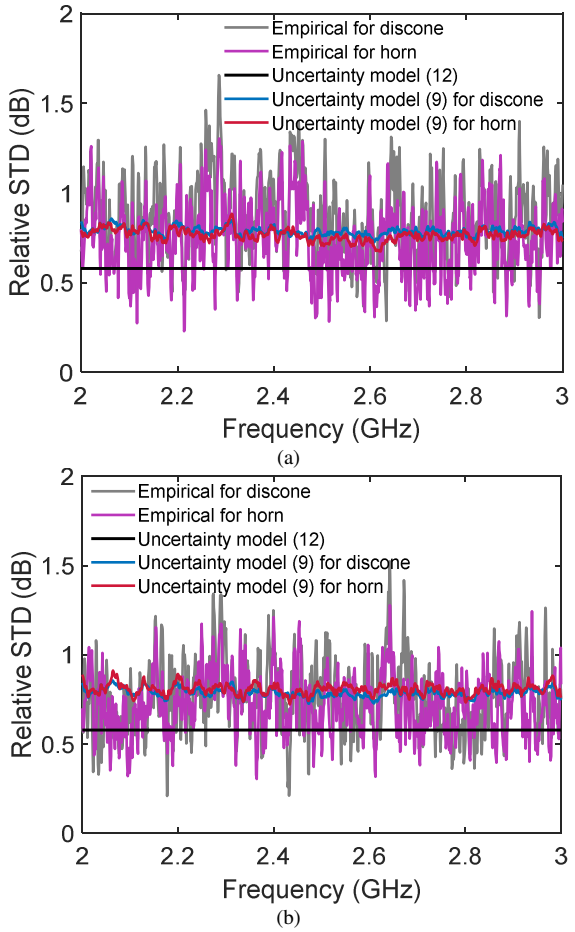

Fig. 8 Empirical and analytical relative uncertainties of the discone and the horn antennas in a loaded RC when using (a) a horn antenna and (b) a discone antenna as the reference antenna.

In order to have an overall and intuitive comparison between the empirical and analytical uncertainties, the specific values of different models obtained from all measurement configurations are summarized in Table II. Specifically, the empirical uncertainty and the K_{avg}-based uncertainty are averaged over the whole testing bandwidth. The ideal theoretical uncertainty is also listed, which is a constant regardless of the measurement configuration. Considering the stochastic nature of RC-based measurements, we will focus on the mean value. For an unloaded RC, the uncertainty model (12) provides a slight underestimation of the empirical values, and the corresponding gap is below 0.1 dB. By comparison, the uncertainties calculated using (9) are comparable to the empirical values, and the corresponding gap is below 0.04 dB. When the RC is loaded with absorbers, both the empirical and the K_{avg}-based uncertainties increase. Moreover, they are still comparable to each other and the corresponding gap is below 0.05 dB. However, the gap between the uncertainty model (12) and the empirical value increases to about 0.2 dB. Even though the uncertainty model (12) performs well with the well-stirred RC, utilizing only the number of independent samples cannot cope with the measurements conducted in the loaded RC. Obviously, additional parameters reflecting the RC's loading condition should be taken into consideration in order to improve the uncertainty model. Overall, it can be concluded that the uncertainty model (9) performs well for both the unloaded and loaded RC.

TABLE II
SPECIFIC VALUES OF THE MEASUREMENT UNCERTAINTIES CALCULATED USING UNCERTAINTY MODEL (9), (12), AND THE EMPIRICAL EFFICIENCIES

Loading Condition	AUT	RA [a]	Averaged Empirical Value (dB)	Averaged Model (9) (dB)	Model (12) (dB)
Unloaded	Horn	Horn	0.66	0.70	0.58
		Discone	0.63	0.67	0.58
	Discone	Horn	0.68	0.71	0.58
		Discone	0.67	0.70	0.58
Loaded With 6 Absorbers	Horn	Horn	0.75	0.77	0.58
		Discone	0.73	0.78	0.58
	Discone	Horn	0.80	0.79	0.58
		Discone	0.77	0.81	0.58

[a] RA represents the reference antenna.

For the reference antenna method, the reference measurement aims to characterize the PTF of the RC. Therefore, in order to have an accurate estimation of the PTF, one may suppose that the reference antenna should better have the same radiation characteristic as the AUT. In this work, for both the horn and the discone AUT, reference measurements are performed using a different horn and discone antennas. Combining Figs. 7 and 8, it can be seen that for a specific AUT, the measurement uncertainties are almost the same regardless of the type of reference antenna used. Moreover, for both unloaded and loaded RCs, the measurement uncertainties are always comparable to each other no matter the similarity between the radiation characteristics of the reference antenna and of the AUT. In other words, the selection of the reference antenna has little effect on the measurement uncertainty. This is quite useful for measurements requiring to characterize the PTF, e.g. measurement of efficiency using the reference antenna method, or measurement of total radiated power and of total isotropic sensitivity using the standard RC methods [8]. This is especially true for some active devices under test, whose radiation characteristics cannot be easily determined.

D. Discussions

It is well known in practice, the measurement uncertainty can be estimated from a sufficient number of independent

This article has been accepted for publication in a future issue of this journal, but has not been fully edited. Content may change prior to final publication. Citation information: DOI 10.1109/TIM.2021.3132991, IEEE Transactions on Instrumentation and Measurement

measurements in practice. From the perspective of statistics, a larger number of independent realizations normally leads to a higher accuracy, i.e. a reduction in the estimated uncertainty. Obviously, the assessment procedure is rather time-consuming. More importantly, for a specific measurand or device under test, the uncertainties estimated through the assessment procedure with a finite number of measurements will be generally different. Considering the stochastics property, we cannot confirm which one is more accurate or representative.

The average K-factor-based uncertainty model can be utilized to determine the measurement uncertainty for a given RC configuration in an efficient and convenient way. Specifically, the uncertainty model requires the number of independent samples and average K-factor only. Once the required parameters are estimated through a single measurement, the measurement uncertainty can be easily determined. Compared with the traditional assessment procedure, the proposed average K-factor-based uncertainty model improves the measurement efficiency and convenience.

It is worth stressing that the uncertainty model introduced in Section II.C can determine the measurement uncertainty using only the number of independent samples. However, it is derived under the assumption of a well-stirred RC, which limits its scope of application. As shown (and analyzed) in Section III.C, it provides an underestimation of the empirical uncertainty in a non-ideal RC environment. By comparison, the average K-factor-based uncertainty model takes the RC's imperfections into consideration; as a result, it performs well regardless of the loading conditions in the RC. In the industry, and in real world, RCs are definitely non-ideal. Thus the average K-factor-based uncertainty model is more suitable and stable. In addition, a single uncertainty model that can cope with different loading conditions is convenient in practice.

It should be noted that a meaningful uncertainty analysis has been established based on an effective measurement. On the other hand, any uncertainty estimator is applicable under specific conditions, e.g., the theoretical uncertainty model requires an ideal Rayleigh distribution. The K-factor-based uncertainty model is valid for practical RC loading or K-factor. Of course, the uncertainty model does not hold for extremely loaded RC (e.g., to the extreme case of an anechoic chamber). This is because two basic requirements of RC-based measurements are not satisfied in such an RC: 1) it becomes increasingly difficult to create high electromagnetic field strength with normal power injection; 2) the measured samples become highly correlated. In general, it may not be possible to provide a specific validity range for the K-factor based uncertainty model. Instead, it is just required that the measurement should be performed in a normally operating RC. An effective RC-based measurement guarantees acceptable K-factor and, therefore, the validity of the K-factor-based uncertainty model. Nevertheless, in order to facilitate the uncertainty analysis, we provide the common range of synthetic uncertainty ($\tilde{u}_{K_{avg}}[\eta_{\mathrm{AUT}}]$) and each component ($\tilde{u}[X]$ and $\tilde{u}[Y]$), which are determined by the K-factor and the number of independent stirring samples in practice. Similar to the analyses in Section II.C and without loss of generality, two case studies are considered, i.e., case study 1 ($K_{avg,\mathrm{REF}} = K_{avg,\mathrm{AUT}}$) and case study 2 ($K_{avg,\mathrm{REF}} = 1.2 \times K_{avg,\mathrm{AUT}}$). It is worth noting that the differences between the K-factors determined by the reference antenna and the AUT may not be too significant, a coefficient of 1.2 is adopted here. The corresponding uncertainties are summarized in Table III.

TABLE III
THE COMMON RANGE OF SYNTHETIC UNCERTAINTY ($\tilde{u}_{K_{avg}}[\eta_{\mathrm{AUT}}]$) AND EACH COMPONENT ($\tilde{u}[X]$ and $\tilde{u}[Y]$) CALCULATED FROM TWO CASE STUDIES WHEN $K_{avg,\mathrm{AUT}} \in [0.05,\ 0.7]$

Case Study	N_{M}	N_{S}	$\tilde{u}[X]$ (dB)	$\tilde{u}[Y]$ (dB)	$\tilde{u}_{K_{avg}}[\eta_{\mathrm{AUT}}]$ (dB)
1	10	10	[0.418, 0.641]	[0.418, 0.641]	[0.580, 0.881]
		10^3	[0.044, 0.069]	[0.044, 0.069]	[0.062, 0.097]
	10^3	10	[0.078, 0.533]	[0.078, 0.533]	[0.110, 0.736]
		10^3	[0.008, 0.056]	[0.008, 0.056]	[0.011, 0.079]
2	10	10	[0.418, 0.641]	[0.425, 0.694]	[0.585, 0.917]
		10^3	[0.044, 0.069]	[0.044, 0.075]	[0.062, 0.101]
	10^3	10	[0.078, 0.533]	[0.088, 0.587]	[0.117, 0.773]
		10^3	[0.008, 0.056]	[0.009, 0.062]	[0.012, 0.084]

Note that the uncertainties are rather small when $N_{\mathrm{M}} \times N_{\mathrm{S}} = 10^6$, therefore, all the uncertainties are retained to last three decimal points to ensure the consistency and effectiveness of the results.

It can be seen from Table III that as $N_{\mathrm{M}} \times N_{\mathrm{S}}$ increases from 10^2 to 10^6, the synthetic uncertainty decreases from [0.58, 0.88] dB to [0.01, 0.08] dB for case study 1, and decreases from [0.59, 0.92] dB to about [0.01, 0.08] dB for case study 2. As expected, the synthetic uncertainty of case study 2 is larger than the counterpart of case study 1. However, the discrepancies are not significant due to the utilization of coefficient 1.2. Combining Tables II and III, it can be observed that the empirical averaged synthetic uncertainties are within the provided ranges. In practical measurements, the provided ranges can be used as references for a rough uncertainty analysis. Of course, one can modify the ranges according to specific conditions, e.g., the practical K-factors and number of independent stirring samples.

IV. CONCLUSIONS

In this work, the average K-factor-based uncertainty model for the standard reference antenna method has been proposed. Extensive efficiency measurements were performed for different RC configurations. For both directional and omnidirectional antennas under test, the empirical relative uncertainties were in accordance with those calculated using the proposed uncertainty model, regardless of the RC's loading condition. The proposed uncertainty model provided an accurate estimation of the measured efficiency using the standard reference antenna method for both loaded and unloaded RC. In addition, it was experimentally verified that the differences in radiation characteristics between the

reference antenna and the AUT had little effect on the measurement uncertainty, making the selection of the reference antenna much more flexible. This finding could also be useful for other RC measurements requiring to characterize the power transfer function.

REFERENCES

[1] V. Rajamani, C. F. Bunting, J. C. West, "Stirred-mode operation of reverberation chambers for EMC testing," *IEEE Trans. Instrum. Meas*., vol. 61, no. 10, pp. 2759-2764, Oct. 2012.

[2] M. G. Becker, M. Frey, S. Streett, et al., "Correlation-based uncertainty in loaded reverberation chambers," *IEEE Trans. Antennas Propag*., vol. 66, no. 10, pp. 5453-5463, Oct. 2018.

[3] J. C. West and C. F. Bunting, "Effects of Frequency Stirring on Reverberation Chamber Testing: An Analysis as a Radiation Problem," *IEEE Trans. Electromagn. Compat*., vol. 61, no. 4, pp. 1345-1352, Aug. 2019.

[4] G. Andrieu and N. Ticaud, "Performance comparison and critical examination of the most popular stirring techniques in reverberation chambers using the 'well-stirred' condition method," *IEEE Trans. Electromagn. Compat*., vol. 62, no. 1, pp. 3-15, Feb. 2020.

[5] D. A. Hill, Electromagnetic Fields in Cavities: Deterministic and Statistical Theories. Hoboken, NJ, USA: Wiley, 2009.

[6] Electromagnetic Compatibility (EMC)-Part 4-21: Testing and Measurement Techniques-Reverberation Chamber Test Methods, Standard IEC 61000-4-21, International Electrotechnical Commission, 2011.

[7] V. M. Primiani, et al., "Reverberation chambers for testing wireless devices and systems," *IEEE Electromagn. Compat*. Mag., vol. 9, no. 2, pp. 45-55, 2020.

[8] Test Plan for Wireless Large-Form-Factor Device Over-the-Air Performance, CTIA Certification, Washington, DC, USA, 2016.

[9] W. Xue, F. Li, X. Chen, S. Zhu, A. Zhang, and T. Svensson, "A unified approach for uncertainty analyses for total radiated power and total isotropic sensitivity measurements in reverberation chamber," *IEEE Trans. Instrum. Meas*., vol. 70, pp. 1-12, 2021.

[10] C. L. Holloway, H. A. Shah, R. J. Pirkl, W.F. Young, D. A. Hill, J. Ladbury, "Reverberation chamber techniques for determining the radiation and total efficiency of antennas," *IEEE Trans. Antennas Propag*., vol. 60, no. 4, pp. 1758–1770, Apr. 2012.

[11] G. Le Fur, P. Besnier, A. Sharaiha, "Time Reversal Efficiency Measurement in Reverberation Chamber," *IEEE Trans. Antennas Propag*., vol. 60, no. 6, pp. 2921-2928, Jun. 2012.

[12] A. Khaleghi, "Time-Domain Measurement of Antenna Efficiency in Reverberation Chamber," *IEEE Trans. Antennas Propag*., vol. 57, no. 3, pp. 817-821, Mar. 2009.

[13] P. Besnier, J. Sol, A. Presse, C. Lemoine, A.C. Tarot, "Antenna Efficiency Measurement from Quality Factor Estimation in Reverberation Chamber," in *Proc. 46th European Microwave Conference (EuMC)*, London, 2016, pp. 715-718.

[14] D. Senic, D.F. Williams, K.A. Remley, C.M. Wang, C.L. Holloway, et al., "Improved Antenna Efficiency Measurement Uncertainty in a Reverberation Chamber at Millimeter-Wave Frequencies," *IEEE Trans. Antennas Propag*., vol. 65, no. 8, pp. 4209-4219, Aug. 2017.

[15] P. Hallbjörner, "Reflective antenna efficiency measurements in reverberation chambers," *Microw. Opt. Technol. Lett*., vol. 30, no. 5, pp. 332-335, 2001.

[16] A. Gifuni, I. D. Flintoft, S. J. Bale, G. C. R. Melia, and A. C. Marvin, "A theory of alternative methods for measurements of absorption cross section and antenna radiation efficiency using nested and contiguous reverberation chambers," *IEEE Trans. Electromagn. Compat.*, vol. 58, no. 3, pp. 678-685, Jun. 2016.

[17] Z. Tian, Y. Huang and Q. Xu, "Enhanced backscatter coefficient measurement at high frequencies in reverberation chamber," 2017 International Workshop on Electromagnetics: Applications and Student Innovation Competition, 2017, pp. 166-167.

[18] L. A. Bronckers, A. Roc'h and A. B. Smolders, "Reverberation Chamber Enhanced Backscattering: High-Frequency Effects," 2019 International Symposium on Electromagnetic Compatibility - EMC EUROPE, 2019, pp. 1-6.

[19] X. Chen, "Measurement uncertainty of antenna efficiency in a reverberation chamber," *IEEE Trans. Electromagn. Compat*., vol. 55, no. 6, pp. 1331-1334, Dec. 2013.

[20] X. Chen, "On statistics of the measured antenna efficiency in a reverberation chamber," *IEEE Trans. Antennas Propag*., vol. 61, no. 11, pp. 5417-5424, Nov. 2013.

[21] W. Xue, X. Chen, M. Zhang, L. Zhao, A. Zhang and Y. Huang, "Statistical Analysis of Antenna Efficiency Measurements with Non-Reference Antenna Methods in a Reverberation Chamber," *IEEE Access*, vol. 8, pp. 113967-113980, 2020.

[22] Q. Xu, L. Xing, Y. Zhao, T. Jia, Y. Huang, "Probability distributions of three-antenna efficiency measurement in a reverberation chamber", *IET Microw., Antennas Propag*., vol. 15, no. 12, pp. 1545-1552, Oct. 2021.

[23] Z. Chen, N. Yang, Y.-X. Guo and M. Y. W. Chia, "An investigation into measurement of handset antennas," *IEEE Trans. Instrum. Meas*., vol. 54, no. 3, pp. 1100-1110, Jun. 2005.

[24] P.-S. Kildal, X. Chen, C. Orlenius, M. Franzén, and C. S. L. Patané, "Characterization of reverberation chambers for OTA measurements of wireless devices: Physical formulations of channel matrix and new uncertainty formula," *IEEE Trans. Antennas Propag*., vol. 60, no. 8, pp. 3875-3891, Aug. 2012.

[25] K. A. Remley, R. J. Pirkl, H. A. Shah, and C.-M. Wang, "Uncertainty from choice of mode-stirring technique in reverberation-chamber measurements," *IEEE Trans. Electromagn. Compat*., vol. 55, no. 6, pp. 1022– 1030, Dec. 2013.

[26] K. A. Remley, C. J. Wang, D. F. Williams, et al., "A Significance Test for Reverberation-Chamber Measurement Uncertainty in Total Radiated Power of Wireless Devices," *IEEE Trans. Electromagn. Compat*., vol. 58, no. 1, pp. 207-219, Feb. 2016.

[27] X. Chen, P. S. Kildal, and S. H. Lai, "Estimation of average Rician K-factor and average mode bandwidth in loaded reverberation chamber," *IEEE Antennas Wireless Propag. Lett*., vol. 10, pp. 1437-1440, 2011.

[28] B. N. Taylor and C. E. Kuyatt, Guidelines for Evaluating and Expressing the Uncertainty of NIST Measurement Results, Gaithersburg, MD, USA: National Institute of Standards and Technology, 1994.

[29] C. Lemoine, E. Amador and P. Besnier, "On the K-Factor Estimation for Rician Channel Simulated in Reverberation Chamber," *IEEE Trans. Antennas Propag*., vol. 59, no. 3, pp. 1003-1012, Mar. 2011.

[30] C. L. Holloway, D. A. Hill, J. M. Ladbury, P. F. Wilson, G. Koepke and J. Coder, "On the Use of Reverberation Chambers to Simulate a Rician Radio Environment for the Testing of Wireless Devices," *IEEE Trans. Antennas Propag*., vol. 54, no. 11, pp. 3167-3177, Nov. 2006.

[31] J. C. West, R. Bakore, and C. F. Bunting, "Statistics of the current induced within a partially shielded enclosure in a reverberation chamber," *IEEE Trans. Electromag. Compat*., vol. 59, no. 6, pp. 2014-2022, Dec. 2017.

[32] X. Chen, P.-S. Kildal, C. Orlenius, and J. Carlsson, "Channel sounding of loaded reverberation chamber for over-the-air testing of wireless devices: Coherence bandwidth versus average mode bandwidth and delay spread," *IEEE Antennas Wireless Propag. Lett.*, vol. 8, pp. 678–681, 2009.